

Effective Control Strategies for Rotary Inverted Pendulum System: Energy-Based, Linear Quadratic Regulator, and Hierarchical Sliding Mode Control Techniques

Duc-Binh Pham, Quy-Thinh Dao, Thi-Van-Anh Nguyen*

Hanoi University of Science and Technology, Ha Noi, Vietnam

*Corresponding author email: anh.nguyenthivan1@hust.edu.vn

Abstract

This work presents a comprehensive study of control problem for the rotary inverted pendulum (RIP), a challenging underactuated system with potential applications in robotics and aerospace. The paper develops effective swing-up energy-based control and stabilization task. It also presents two controllers, linear quadratic regulator (LQR) and hierarchical sliding mode control (HSMC), that effectively handle the stabilization problem. System modelling is based on Lagrangian mechanics, and the control strategies are evaluated using simulations and compared in terms of performance and robustness. The results demonstrate that energy-based control is effective for swing-up, while linear quadratic regulator and hierarchical sliding mode control are effective for stabilization. The proposed controllers show promising results and contribute to the development of robust and efficient control strategies for the rotary inverted pendulum system. The study has implications for the development of control strategies for other underactuated systems and can potentially lead to advancements in the field of robotics and aerospace.

Keywords: Rotary inverted pendulum, swing-up and stabilization control, energy-based control, hierarchical sliding mode control, linear quadratic regulator.

1. Introduction

Underactuated systems are a type of nonlinear system that require advanced control techniques due to having fewer control inputs than degrees of freedom. A well-known instance of an underactuated system is the rotary inverted pendulum (RIP), which consists of a pendulum attached to a motorized arm. The challenge of controlling this object is to keep the pendulum balanced in the upright position while simultaneously controlling the rotation of the arm.

The RIP has significant applications in the field of robotics, particularly in developing control strategies and motion planning algorithms for two-wheeled robots like Segways [1, 2]. The dynamics models are similar, making it an ideal testbed for developing and testing control strategies for these types of robots. Researchers can use the rotary inverted pendulum to study the effects of different control inputs and algorithms on the system's stability and performance. This can lead to the development of more efficient and robust control strategies for two-wheeled robots, which can be used in various applications, such as transportation, military operations, and aerospace.

The rotary inverted pendulum is a complex and challenging system to control due to its nonlinear and underactuated dynamics. The control of the RIP system typically involves two main control tasks:

swing-up and stabilization [3-5]. Swing-up is the process of bringing the pendulum from the rest position to the upright position, while stabilization process keeps pendulum in equilibrium position. These two tasks require different control strategies due to the distinct nature of the control problem.

A popular approach for swinging up this type of pendulum is the use of nonlinear control techniques such as energy-based control [6], feedback linearization control or sliding mode control [7] and so on. Energy-based control involves shaping the energy of the system such that it reaches a desired state, while feedback linearization control involves transforming the system dynamics into a linear form that can be more easily controlled using linear strategies. Another advanced control technique for swinging up the RIP is the implementation of model predictive control (MPC), as presented in [8].

Keeping the RIP stable is another important task in control theory. Several techniques for controlling the system have been developed, comprising both linear and nonlinear approaches. Linear control methods such as Linear Quadratic Regulator (LQR) control [9] and proportional-integral-derivative (PID) control can be used to keep the pendulum stable in the equilibrium point. Nonlinear control methods such as adaptive control [10], backstepping control [11], and advanced sliding mode control [12], are also effective

in stabilizing the rotary inverted pendulum. Adaptive control can adapt to uncertainties and disturbances, while backstepping control can recursively design control inputs to stabilize the system dynamics. Hierarchical sliding mode control (HSMC) is another nonlinear control technique that has been used to stabilize the rotary inverted pendulum. HSMC demonstrates superior performance compared to other control methods in dealing with external disturbances and uncertainties.

This paper discusses research conducted on controlling the (RIP) system. Section 2 presents the system modelling, where the dynamic equations of the system are derived using Euler - Lagrange equations. Section 3 discusses various control methods for both swing-up and stabilization tasks, including energy-based control, hierarchical sliding mode control techniques, and linear quadratic regulator. Section 4 shows the simulations and results, where the performance of the different control strategies is evaluated and compared. Finally, Section 5 presents the conclusions of the study, summarizing the main findings and highlighting future research directions. The study contributes to the development of effective control strategies for the rotary inverted pendulum system, which has applications in various fields, including robotics and aerospace.

2. System Modelling

The inverted pendulum system consists of the main components such as a DC motor, a rotary arm and a pendulum rod. Initially, we built a mathematical model for the DC motor.

Considering the voltage applied to the motor [13], we have:

$$V_{in} = I_m R_m + L_m \frac{dI_m}{dt} + K_m \dot{\theta}_m \quad (1)$$

where I_m , R_m , L_m are amperage, resistor, and inductance of coil, respectively. K_m is the back EMF constant. Assume that effect of the inductor is negligible, the torque of the motor can be calculated as:

$$T_m = \frac{V_{in} K_m - K_m^2 \dot{\theta}_m}{R_m} \quad (2)$$

Load moment converted to the motor shaft after the gearbox is:

$$T_{out} = T_m k_g \eta_g - J_m k_g^2 \eta_g \ddot{\theta} \quad (3)$$

with the gearbox ratio k_g , gearbox efficient η_g and J_m is the moment of inertia of system after gearbox.

From (2) and (3), the following equation can be derived:

$$T_{out} = \frac{V_{in} K_m - K_m^2 k_g \dot{\theta}}{R_m} k_g \eta_g - J_m k_g^2 \eta_g \ddot{\theta} \quad (4)$$

Having acquired the motor's mathematical model, we proceeded with the RIP modeling. The comprehensive process of modeling the system can be found in [14].

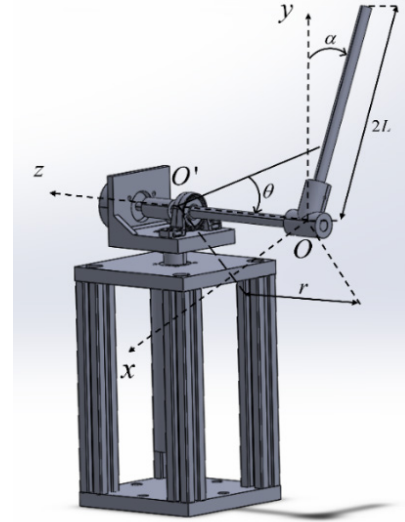


Fig. 1. RIP model

Fig. 1 shows the simple model of the RIP where m (kg) and $2L$ (m) are the mass and length of the pendulum rod. The pendulum rotates around the shaft of the DC motor thanks to the pendulum arm with M (kg) and r (m). The pendulum's angle and the rotation angle of arm are α and θ , respectively. The acceleration due to gravity is g (ms^{-2}). Consider the center of gravity of the pendulum placed in the middle.

Potential energy of the pendulum system:

$$V = mgL \cos(\alpha) \quad (5)$$

Kinetic energy of the pendulum system:

$$T = \frac{1}{2} J_{eq} \dot{\theta}^2 + \frac{1}{2} m (L \sin \alpha (\dot{\alpha}))^2 + \frac{1}{2} m (r \dot{\theta} - L \cos \alpha (\dot{\alpha}))^2 + \frac{1}{6} m L^2 \dot{\alpha}^2 \quad (6)$$

Then the Lagrangian is obtained as below:

$$L = \frac{1}{2} J_{eq} \dot{\theta}^2 + \frac{2}{3} m L^2 \dot{\alpha}^2 - m L r \dot{\theta} \cos(\alpha) \dot{\alpha} + \frac{1}{2} m r^2 \dot{\theta}^2 - mgL \cos \alpha \quad (7)$$

Applying Euler – Lagrange equations for α and θ , we have:

$$\begin{cases} \frac{d}{dt} \left(\frac{\partial L}{\partial \dot{\alpha}} \right) - \frac{\partial L}{\partial \alpha} = 0 \\ \frac{d}{dt} \left(\frac{\partial L}{\partial \dot{\theta}} \right) - \frac{\partial L}{\partial \theta} = T_{out} - B_{eq} \dot{\theta} \end{cases} \quad (8)$$

From (7) and (8), the dynamic equation can be calculated:

$$\begin{cases} (J_{eq} + mr^2 + J_m k_g^2 \eta_g) \ddot{\theta} + mLr \cos(\alpha) \ddot{\alpha} \\ + mLr \sin(\alpha) \dot{\alpha}^2 + \left(B_{eq} + \frac{\eta_g k_g^2 K_m^2}{R_m} \right) \dot{\theta} = \frac{K_m k_g \eta_g}{R_m} V_{in} \\ - mLr \cos(\alpha) \ddot{\theta} + \frac{4}{3} mL^2 \ddot{\alpha} - mLg \sin \alpha = 0 \end{cases} \quad (9)$$

These equations can be written as:

$$\begin{cases} b_1 \ddot{\theta} + b_2 \cos(\alpha) \ddot{\alpha} + b_2 \sin(\alpha) \dot{\alpha}^2 + b_5 \dot{\theta} = b_6 V_{in} \\ -b_2 \cos(\alpha) \ddot{\theta} + b_3 \ddot{\alpha} - b_4 \sin \alpha = 0 \end{cases} \quad (10)$$

with

$$b_1 = J_{eq} + mr^2 + J_m k_g^2 \eta_g ;$$

$$b_2 = mLr ;$$

$$b_3 = \frac{4}{3} mL^2 ;$$

$$b_4 = mLg ;$$

$$b_5 = B_{eq} + \frac{\eta_g k_g^2 K_m^2}{R_m} ;$$

$$b_6 = \frac{K_m k_g \eta_g}{R_m} .$$

Linearization model of the inverted pendulum is also obtained:

$$\begin{bmatrix} \dot{\theta} \\ \dot{\alpha} \\ \ddot{\theta} \\ \ddot{\alpha} \end{bmatrix} = \begin{bmatrix} 0 & 0 & 1 & 0 \\ 0 & 0 & 0 & 1 \\ 0 & \frac{b_2 b_4}{b_1 b_3 - b_2^2} & \frac{-b_3 b_5}{b_1 b_3 - b_2^2} & 0 \\ 0 & \frac{b_1 b_4}{b_1 b_3 - b_2^2} & \frac{-b_2 b_3}{b_1 b_3 - b_2^2} & 0 \end{bmatrix} \begin{bmatrix} \theta \\ \alpha \\ \dot{\theta} \\ \dot{\alpha} \end{bmatrix} + \begin{bmatrix} 0 \\ 0 \\ \frac{b_3 b_6}{b_1 b_3 - b_2^2} \\ \frac{b_2 b_6}{b_1 b_3 - b_2^2} \end{bmatrix} V_{in} . \quad (11)$$

3. Control Problem

The RIP's control issue can be categorized into two primary objectives: swing up and stabilization. The first task is to efficiently move the pendulum from its initial position to the vertical upright position. This task requires applying external energy to the system to increase the pendulum's energy until it is sufficient to reach the upright position. Besides, stabilization task involves maintaining the pendulum in the desired position and ensuring that it remains balanced despite any disturbances or external forces acting on it. This task requires controlling the pendulum's movements and applying corrective forces to keep it stable.

3.1. Energy-Based Control and Linear Quadratic Regulator

3.1.1. Energy-based control (EC)

Pendulum motion equation with moment of inertia J_p is written:

$$mL\ddot{\theta} \cos \alpha - mgL \sin \alpha + J_p \ddot{\alpha} = 0 \quad (12)$$

For handling swing up task, it is necessary to supply the pendulum with a sufficient amount of energy. The energy equation of the pendulum in the absence of a control signal can be given as follows:

$$E = \frac{1}{2} J_p \dot{\alpha}^2 + mgL \cos \alpha \quad (13)$$

$$\Rightarrow \frac{dE}{dt} = J_p \dot{\alpha} \ddot{\alpha} - mgL \dot{\alpha} \sin \alpha \quad (14)$$

Multiplying both sides of (12) with $\dot{\alpha}$ and substituting to the above equation yields:

$$\frac{dE}{dt} = -(mL\dot{\alpha} \cos \alpha) \ddot{\theta} \quad (15)$$

The Lyapunov function and the control law can be chosen as:

$$V = \frac{(E - E_0)^2}{2} \quad (16)$$

$$\ddot{\theta} = k(E - E_0) \dot{\alpha} \cos \alpha \quad (17)$$

From (16):

$$\frac{dV}{dt} = (E - E_0) (-(mL\dot{\alpha} \cos \alpha) \ddot{\theta}) \quad (18)$$

Then:

$$\frac{dV}{dt} = -mkL((E - E_0) \dot{\alpha} \cos \alpha)^2 < 0 \quad (19)$$

And the system is proven to be stable.

The control law can be provided where ξ is the maximum acceleration of the motor:

$$\ddot{\theta} = \xi \text{sign}((E - E_0)\dot{\alpha} \cos \alpha) \quad (20)$$

However, when energy E approaches E_0 or $|E - E_0|$ approaches zero, control law (20) will cause chattering phenomenon. To solve this problem, the following control law with the saturation function is utilized instead of (20):

$$\ddot{\theta} = \text{sat}_{\xi}(k(E - E_0)\text{sign}(\dot{\alpha} \cos \alpha)) \quad (21)$$

The real control signal applied to the motor is voltage, then the relationship between $\ddot{\theta}$ and V_{in} is given as:

$$V_{in} = \frac{RML\ddot{\theta}}{\eta_g k_g k_m^2} + k_g k_m \dot{\theta}. \quad (22)$$

As shown in Fig. 2 and 3, the swing up EC controller has successfully brought the pendulum to the desired position through continuously reversing the motor.

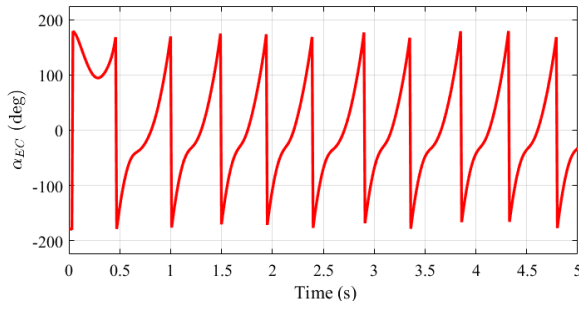


Fig. 2. Pendulum's angle with EC controller

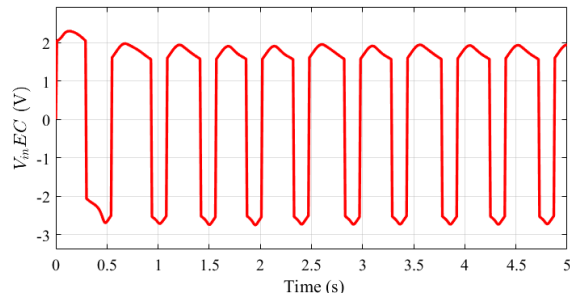


Fig. 3. Applied voltage with EC controller

3.1.2. Linear quadratic regulator

Once a swing up controller has been developed for the rotary inverted pendulum, the next step is to design a stabilization controller to maintain the pendulum in an upright position. Depending on the system's specific characteristics, the stabilization controller can be either nonlinear or linear. One commonly used linear controller for stabilization is the linear quadratic regulator (LQR). The LQR is a

feedback control algorithm that aims to minimize a quadratic cost function:

$$J = \int_0^{t_f} (x(t)^T Q x(t) + u(t)^T R u(t)) dt + x(t_f)^T M x(t_f) \quad (23)$$

where R is a positive definite matrix; M and Q are positive semi-definite matrices. Define the value V as:

$$V = \min_{u(t)} J(x(t), u(t), t_0, t_f) \quad (24)$$

We have the Hamilton–Jacobi–Bellman equation:

$$-\frac{\partial V}{\partial t} = \min_{u(t)} \left(\frac{\partial V^T}{\partial x^T} (Ax + Bu) + x(t)^T Q x(t) + u(t)^T R u(t) \right) \quad (25)$$

Consider the value function V :

$$V(x, t) = x^T S(t)x \quad (26)$$

with $S(t)$ is a positive definite matrix $S(t) = S^T(t) > 0$.

LQR control signal is derived with the $S(t)$ matrix satisfying the Riccati differential in (28):

$$u = -R^{-1} B^T S(t)x = -Kx \quad (27)$$

$$\dot{S}(t) = Q + S(t)A - S(t)BR^{-1}B^T S(t) + A^T S(t) \quad (28)$$

From the linearization model (11) and chosen matrices Q and R as

$$Q = \begin{bmatrix} 1 & 0 & 0 & 0 \\ 0 & 50 & 0 & 0 \\ 0 & 0 & 50 & 0 \\ 0 & 0 & 0 & 1 \end{bmatrix}, \quad R = 1$$

the feedback controller is obtained:

$$K = [-0.0200 \quad 7.1535 \quad -0.2100 \quad 1.0258].$$

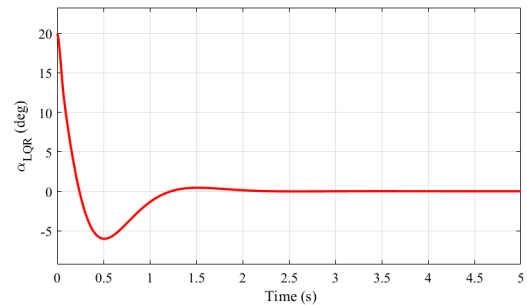


Fig. 4. Pendulum's angle with LQR controller

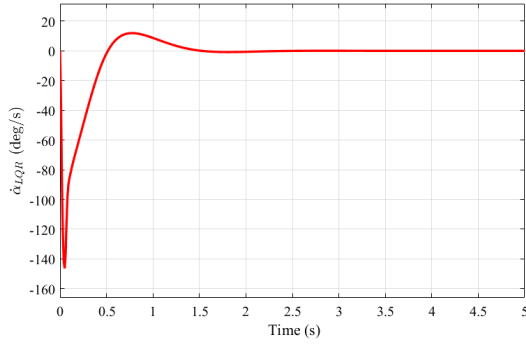


Fig. 5. Pendulum's speed with LQR controller

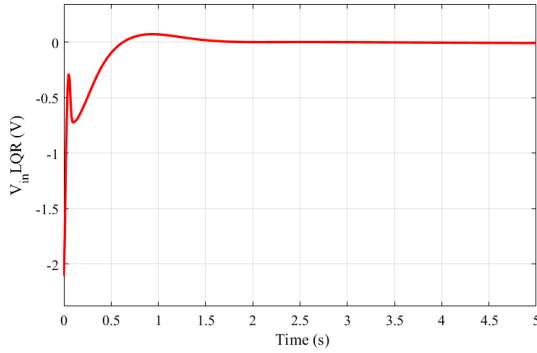


Fig. 6. Applied voltage with LQR controller

Fig. 4, 5, and 6 demonstrate that the LQR linear controller was effective in stabilizing the pendulum with a small initial angle.

3.2. Hierarchical Sliding Mode Control

3.2.1. Control law

Although the linear quadratic regulator is a popular controller for stabilizing the RIP, it has limitations due to its linear nature. LQR requires the linearization of the nonlinear system, which may not be accurate in practice. Therefore, in practice, it is better to use a nonlinear controller for stabilization, especially for the rotary inverted pendulum system. A possible alternative to LQR is the hierarchical sliding mode control (HSMC) technique, which is very effective for this kind of underactuated system. We first rewrite the inverted pendulum model in the form of:

$$\begin{cases} \dot{x}_1 = x_2 \\ \dot{x}_2 = F_1(x) + G_1(x)u \\ \dot{x}_3 = x_4 \\ \dot{x}_4 = F_2(x) + G_2(x)u \end{cases} \quad (29)$$

with $[x_1 \ x_2 \ x_3 \ x_4] = [\alpha \ \dot{\alpha} \ \theta \ \dot{\theta}]$ and

$$F_1(x) = \frac{b_1 b_4 \sin(x_1) - b_2 \cos(x_1) (b_2 \sin(x_1) x_2^2 + b_3 x_4)}{b_1 b_3 - b_2^2 \cos(x_1)^2};$$

$$G_1(x) = \frac{b_6 b_2 \cos(x_1)}{b_1 b_3 - b_2^2 \cos(x_1)^2};$$

$$F_2(x) = \frac{b_3 F_1(x) - b_4 \sin(x_1)}{b_2 \cos(x_1)};$$

$$G_2(x) = \frac{b_6 b_3}{b_1 b_3 - b_2^2 \cos(x_1)^2}$$

It can be seen that the rotary inverted pendulum system can be divided into two subsystems, respectively the arm attached to the motor shaft and the pendulum rod. We construct the sliding surfaces for each subsystem:

$$s_1 = x_2 + \lambda_1 x_1 \quad (30)$$

$$s_2 = x_4 + \lambda_2 x_3$$

Taking the derivatives of these sliding surfaces with respect to time gives:

$$\dot{s}_1 = \dot{x}_2 + \lambda_1 \dot{x}_1 = \lambda_1 x_2 + F_1 + G_1 u \quad (31)$$

$$\dot{s}_2 = \dot{x}_4 + \lambda_2 \dot{x}_3 = \lambda_2 x_4 + F_2 + G_2 u$$

Let $\dot{s}_1 = \dot{s}_2 = 0$, the equivalent control signal for each subsystem can be inferred as:

$$u_{eq1} = -\frac{\lambda_1 x_2 + F_1}{G_1} \quad (32)$$

$$u_{eq2} = -\frac{\lambda_2 x_4 + F_2}{G_2}$$

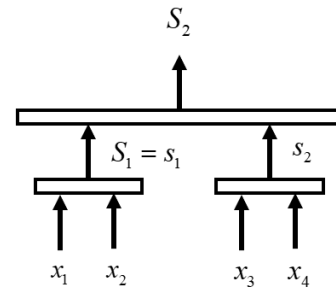


Fig. 7. Hierarchical structure of sliding surface

Fig. 7 illustrates the hierarchical arrangement of the sliding surfaces where the first layer is the sliding manifold of the first subsystem, so we have $S_1 = s_1$. The integration of the sliding surface from the second subsystem s_2 and the first subsystem yields the sliding surface for the entire system, denoted as S_2 . With this representation, the total sliding surface of the whole system will carry the information of all the different sub-sliding surfaces and layers. We can represent the sliding surface S_2 as follows:

$$S_2 = k_1 S_1 + s_2 \quad (33)$$

where k_1 is a chosen constant. Control signal of the whole system can be synthesized:

$$u = u_{eq_1} + u_{eq_2} + u_{sw} \quad (34)$$

The u_{sw} component helps to bring the system to a specified sliding manifold. To determine the u_{sw} , the following Lyapunov function is considered:

$$V(t) = \frac{1}{2} S_2^2 \quad (35)$$

Take the derivative of the Lyapunov function and substitute values from (31) and (33), we have:

$$\begin{aligned} \dot{V} &= S_2 \dot{S}_2 = S_2 (k_1 \dot{S}_1 + \dot{s}_2) \\ &= S_2 [k_1 (\lambda_1 \dot{x}_1 + \dot{x}_2) + (\lambda_2 \dot{x}_3 + \dot{x}_4)] \\ &= S_2 \left[k_1 (\lambda_1 x_2 + F_1 + G_1 (u_{eq_1} + u_{eq_2} + u_{sw})) \right. \\ &\quad \left. + (\lambda_2 x_4 + F_2 + G_2 (u_{eq_1} + u_{eq_2} + u_{sw})) \right] \end{aligned} \quad (36)$$

Let $\dot{S}_2 = -kS_2 - \eta \text{sgn}(S_2)$ where k and η are positive scalar, the u_{sw} can be calculated as:

$$u_{sw} = -\frac{G_2}{k_1 G_1 + G_2} u_{eq_1} - \frac{k_1 G_1}{k_1 G_1 + G_2} u_{eq_2} - \frac{kS_2 + \eta \text{sgn}(S_2)}{k_1 G_1 + G_2} \quad (37)$$

The control signal of the whole system is:

$$\begin{aligned} u &= u_{sw} + u_{eq_1} + u_{eq_2} \\ &= \frac{k_1 G_1}{k_1 G_1 + G_2} u_{eq_1} + \frac{G_2}{k_1 G_1 + G_2} u_{eq_2} - \frac{kS_2 + \eta \text{sgn}(S_2)}{k_1 G_1 + G_2} \end{aligned} \quad (38)$$

3.2.2. Stability Analysis

From the Lyapunov function in (35), we have the time derivative of V :

$$\begin{aligned} \dot{V} &= S_2 \dot{S}_2 \\ &= S_2 (-kS_2 - \eta \text{sgn}(S_2)) \\ &= -kS_2^2 - \eta |S_2|. \end{aligned} \quad (39)$$

Integrate both sides of (39):

$$\int_0^t \dot{V} d\tau = \int_0^t (-kS_2^2 - \eta |S_2|) d\tau \quad (40)$$

With $V(t) > 0$, we have:

$$\lim_{t \rightarrow \infty} \int_0^t (kS_2^2 + \eta |S_2|) d\tau \leq V(0) < \infty \quad (41)$$

Based on the Barbalat's lemma, the following equation is inferred:

$$\lim_{t \rightarrow \infty} (kS_2^2 + \eta |S_2|) = 0 \quad (42)$$

Then $S_2 \rightarrow 0$ when $t \rightarrow \infty$. The sliding manifold S_2 is proven to be asymptotically stable.

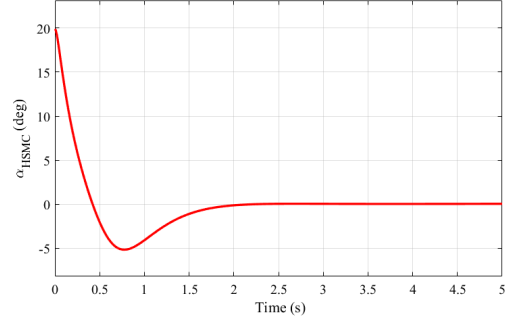


Fig. 8. Pendulum's angle with HSMC controller

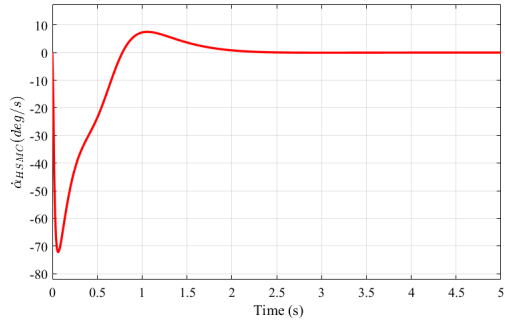


Fig. 9. Pendulum's speed with HSMC controller

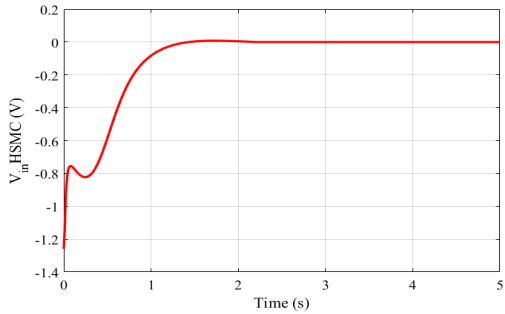


Fig. 10. Applied voltage with HSMC controller

Fig. 8, 9 and 10 are simulation results when using the HSMC controller to balance the pendulum. This nonlinear controller also gave a good response to the same initial conditions as when using LQR .

4. Simulations and Results

Table 1 displays the parameters of the simulated rotary inverted pendulum.

In order to achieve both the swing up and balance control objectives for the inverted pendulum system simultaneously, a hybrid controller involving an energy-based controller and a stabilization controller which could be Linear Quadratic Regulator or Hierarchical Sliding Mode Control is utilized. Fig. 11 is the control architecture diagram for the entire system.

Table 1. Parameters of RIP

Parameter	Notation	Value
Pendulum rod's mass (kg)	m	0.027
Pendulum arm's mass (kg)	M	0.05
Equivalent moment of inertia of the pendulum arm and gears (kgm^2)	J_{eq}	2.33×10^{-4}
Length of the pendulum rod to the center of mass (m)	L	0.153
Pendulum arm's length (m)	r	0.08260
Vicious friction coefficient of the motor (Nms/rad)	B_{eq}	0.0005
Gravitational acceleration (m/s^2)	g	9.81
Motor armature resistance (Ω)	R_m	3.3
Gearbox efficiency	η_g	0.9
Gearbox ratio	k_g	70
Back EMF constant	K_m	0.02797
Rated voltage (V)	V_{rated}	12
Rated current (A)	I_{rated}	0.3
Rated torque (kg.cm)	T_{rated}	0.1
Rated power (W)	P_{rated}	3.6

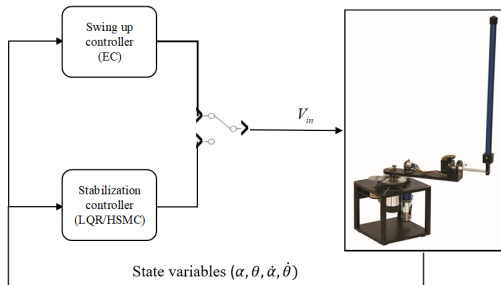


Fig. 11. Control structure

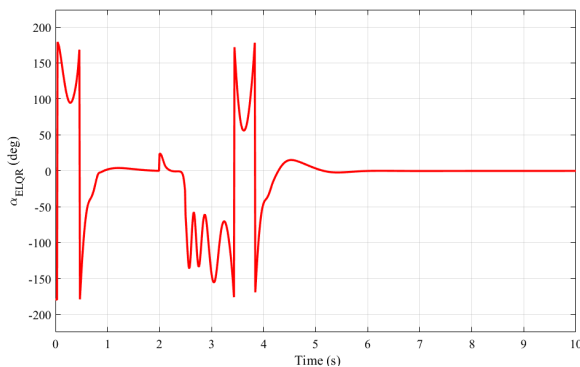


Fig. 12. Pendulum's angle with ELQR controller

When the deflection angle of pendulum rod is small, the switch will be activated to continue taking control signals from the stabilization controller.

The performance of the Energy-Linear Quadratic Regulator controller was evaluated by observing the

deflection angle α of the pendulum, as depicted in Fig. 12. After about one second, the pendulum bar has stabilized after undergoing the processes of oscillation and swing up. To evaluate the controller's effectiveness, a disturbance signal was applied to the pendulum at the 2nd second. Even though an external force has caused the pendulum to oscillate and deviate from its equilibrium position from 2nd to 4th second, the swing up controller has continued to operate and successfully returned the pendulum to the desired position at 6th second, where it stayed stable. The combination of the energy-based swing up control and LQR-based stabilization control has proven to be effective.

The voltage signal applied to the motor in Fig. 13, shows a significant change when the pendulum is suddenly affected by disturbance. The voltage value is quickly pushed to its maximum value to provide the pendulum with enough energy to swing up again.

However, when the pendulum reaches its equilibrium position, the voltage value becomes almost zero. This demonstrates the efficiency of the swing up controller in providing sufficient energy for swing up, and the stabilization controller in maintaining the pendulum's equilibrium position.

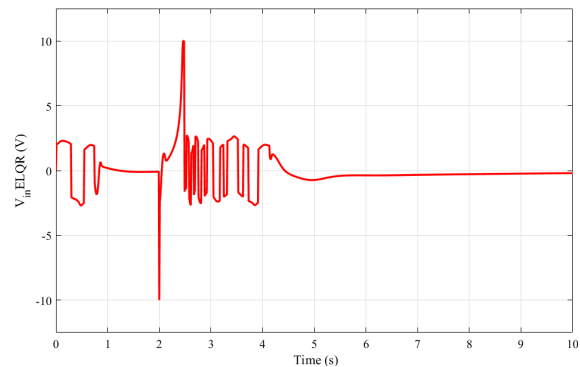


Fig. 13. Applied voltage with ELQR controller

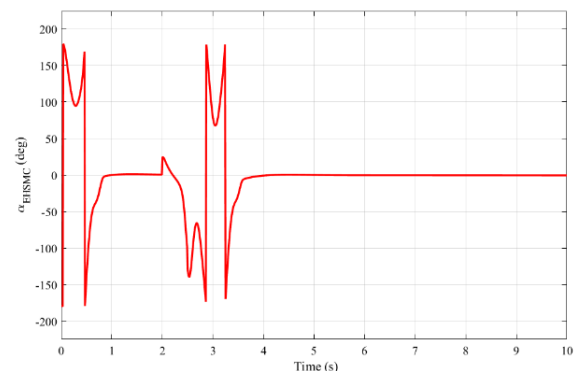


Fig. 14. Pendulum's angle with EHSMC controller

The combined EC and HSMC controller in Fig. 14 has demonstrated its ability to meet the control requirements of the system. The swing up controller quickly brings the pendulum to the zero-angle

asymptote in the early stages, and the pendulum stays balanced in the desired position for one second before starting to oscillate due to the effect of disturbance in the 2nd second. However, the pendulum quickly swings up again in response to the external disturbance. At the fourth second, the deflection angle value of the pendulum returns to zero, indicating that the pendulum has been successfully stabilized once again. The outcomes indicate that the Energy-Hierarchical Sliding Mode Control (EHSMC) controller is efficient in stabilizing the RIP system, even when external disturbances are present.

Similar to the ELQR controller, the voltage in Fig. 15 is relatively small and has a sudden increase when the pendulum is affected by noise. However, the maximum values of voltage when using the EHSMC controller are somewhat smaller and more rapidly decrease to zero.

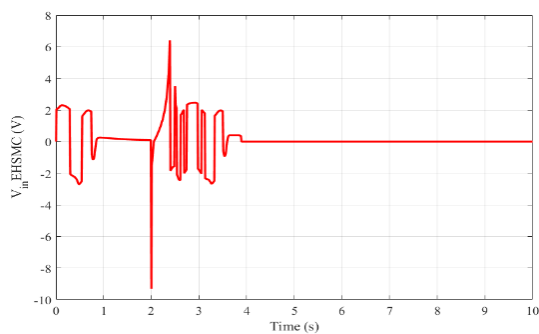


Fig. 15. Applied voltage with EHSMC controller

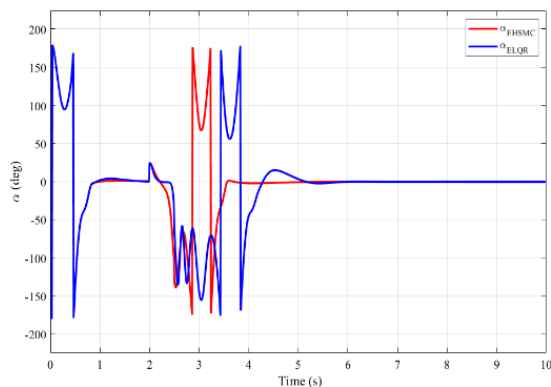


Fig. 16. Comparison of ELQR and EHSMC

In order to compare the effectiveness of EHSMC and ELQR, both controllers were subjected to the same initial angular conditions and disturbance. As depicted in Fig. 16, the blue line (α_{ELQR}) represents the deflection angle of the pendulum when using ELQR, while the red line (α_{EHSMC}) represents EHSMC. It is evident that the responses of the two controllers are relatively similar until the occurrence of disturbance in the second swing up and balance. At this point, EHSMC exhibits a superior response time as the pendulum stabilizes within approximately 2 seconds,

while ELQR takes almost 4 seconds to arrive at this position. Therefore, the combination of EC for swing up and hierarchical sliding mode controller for stabilization was more effective than the combination of energy-based controller and LQR for stabilizing the RIP.

The EHSMC technique, despite its advantages, also has some principal restrictions and disadvantages. One of the main restrictions is the complexity of design and implementation. EHSMC requires the determination of multiple sliding surfaces and corresponding control laws for each hierarchical level, which can increase the computational burden and the design effort. Furthermore, the effectiveness of EHSMC may heavily depend on the tuning of control gains and the selection of sliding surface parameters. Improper tuning or inappropriate selection can lead to suboptimal or unstable control performance.

5. Conclusion

In conclusion, the RIP has been a crucial research subject, not only in theory but also in practical applications. The study of control techniques for this type of pendulum has provided a foundation for the development of various other balancing systems. In this article, the efficiency of the swing up energy-based controller and the stability controllers, including LQR and HSMC, have been demonstrated. The primary control objectives of the RIP system were successfully achieved by integrating the EC controller with the LQR and HSMC controllers. This integration resulted in the development of the ELQR and EHSMC hybrid controllers. Despite the presence of external disturbances, they demonstrate remarkable performance. This study can serve as a reference for further research on the control of similar systems and can also be used in practical applications.

References

- [1] Hoang, U. T. T., Kim, T. D., Le, H. X., Pham, D. X., Phan, M. X., & Nguyen, T. V., Adaptive fuzzy hierarchical sliding mode control for ball segway, *Automatic Control and Computer Sciences*, 56(6), 519-532, 2022. <https://doi.org/10.3103/S0146411622060050>
- [2] Draz, M. U., Ali, M. S., Majeed, M., Ejaz, U., & Izhar, U., Segway electric vehicle. In 2012 International Conference of Robotics and Artificial Intelligence, pp. 34-39, IEEE (2012, October). <https://doi.org/10.1109/ICRAI.2012.6413423>
- [3] Yang, X., & Zheng, X. (2018). Swing-up and stabilization control design for an underactuated rotary inverted pendulum system: Theory and experiments. *IEEE Transactions on Industrial Electronics*, 65(9), 7229-7238. <https://doi.org/10.1109/TIE.2018.2793214>
- [4] Susanto, E., Rahmat, B., & Ishitobi, M., Stabilization of rotary inverted pendulum using proportional derivative and fuzzy controls, In 2022 9th International

- Conference on Information Technology, Computer, and Electrical Engineering (ICITACEE) pp. 34-37, IEEE, <https://doi.org/10.1109/ICITACEE55701.2022.9924142>
- [5] Mathew, N. J., Rao, K. K., & Sivakumaran, N., Swing up and stabilization control of a rotary inverted pendulum. *IFAC Proceedings Volumes*, 46 (32), 654-659, 2013. <https://doi.org/10.3182/20131218-3-IN-2045.00128>
- [6] Chou, K. Y., & Chen, Y. P., Energy based swing-up controller design using phase plane method for rotary inverted pendulum. In *2014 13th International Conference on Control Automation Robotics & Vision (ICARCV)* (pp. 975-979). IEEE, 2014, December. <https://doi.org/10.1109/ICARCV.2014.7064438>
- [7] Kurode, S., Chalanga, A., & Bandyopadhyay, B., Swing-up and stabilization of rotary inverted pendulum using sliding modes. *IFAC Proceedings Volumes*, 44(1), 10685-10690, (2011). <https://doi.org/10.3182/20110828-6-IT-1002.02933>
- [8] Jung, S., & Wen, J. T., Nonlinear model predictive control for the swing-up of a rotary inverted pendulum. *J. Dyn. Sys., Meas., Control*, 126(3), 666-673, 2004. <https://doi.org/10.1115/1.1789541>
- [9] Park, M., Kim, Y. J., & Lee, J. J., Swing-up and LQR stabilization of a rotary inverted pendulum, *Artificial Life and Robotics*, 16, 94-97, 2011. <https://doi.org/10.1007/s10015-011-0897-9>
- [10] Chen, Y. F., & Huang, A. C. Adaptive control of rotary inverted pendulum system with time-varying uncertainties. *Nonlinear Dynamics*, 76, 95-102., 2014. <https://doi.org/10.1007/s11071-013-1112-4>
- [11] Huang, J., Zhang, T., Fan, Y., & Sun, J. Q., Control of rotary inverted pendulum using model-free backstepping technique. *IEEE Access*, 7, 96965-96973, 2019. <https://doi.org/10.1109/ACCESS.2019.2930220>
- [12] Mofid, O., Alattas, K. A., Mobayen, S., Vu, M. T., & Bouteraa, Y., Adaptive finite-time command-filtered backstepping sliding mode control for stabilization of a disturbed rotary-inverted-pendulum with experimental validation. *Journal of Vibration and Control*, 29(5-6), 1431-1446, 2023. <https://doi.org/10.1177/10775463211064022>
- [13] Semenov, A. S., Khubieva, V. M., & Kharitonov, Y. S., Mathematical modeling of static and dynamic modes DC motors in software package MATLAB. In *2018 International Russian Automation Conference, IEEE*, 1-5, 2018, September. <https://doi.org/10.1109/RUSAUTOCON.2018.8501666>
- [14] Rajeswari, K., Vivek, P., & Nandhagopal, J., Swing up and stabilization of rotational inverted pendulum by fuzzy sliding mode controller, In *Emerging Trends in Computing and Expert Technology*, Springer International Publishing, 415-423, 2020. https://doi.org/10.1007/978-3-030-32150-5_40